

Shaker Potassium Channel Gating I: Transitions Near the Open State

TOSHINORI HOSHI, WILLIAM N. ZAGOTTA, and RICHARD W. ALDRICH

From the Department of Molecular and Cellular Physiology, Howard Hughes Medical Institute, Stanford University School of Medicine, Stanford, California 94305

ABSTRACT Kinetics of single voltage-dependent *Shaker* potassium channels expressed in *Xenopus* oocytes were studied in the absence of fast *N*-type inactivation. Comparison of the single-channel first latency distribution and the time course of the ensemble average current showed that the activation time course and its voltage dependence are largely determined by the transitions before first opening. The open dwell time data are consistent with a single kinetically distinguishable open state. Once the channel opens, it can enter at least two closed states which are not traversed frequently during the activation process. The rate constants for the transitions among these closed states and the open state are nearly voltage-independent at depolarized voltages (> -30 mV). During the deactivation process at more negative voltages, the channel can close directly to a closed state in the activation pathway in a voltage-dependent fashion.

INTRODUCTION

Voltage-dependent ion channels respond to changes in the electric field across the membrane by undergoing conformational changes that open an ion permeable pore. This activation process requires a number of conformational transitions in the channel protein. The voltage dependence in the activation process is caused by the rearrangements of charges or dipoles within the channel protein associated with some of the conformational transitions. These intramolecular charge movements make the conformational transition rates voltage-dependent and can be directly measured as gating currents (Armstrong, 1981; Bezanilla, 1985).

An important goal of ion channel research is to understand the molecular mechanisms of the conformational changes involved in channel gating. The molecular mechanism that underlies these conformational changes remains unclear. Recently cDNA clones have been isolated and the primary structure determined for a

Dr. Hoshi's present address is Department of Physiology and Biophysics, University of Iowa, Iowa City, Iowa 52242-1109.

Dr. Zagotta's present address is Department of Physiology and Biophysics, SJ-40, University of Washington, Seattle, Washington 98195.

Address correspondence to Richard W. Aldrich, Department of Molecular and Cellular Physiology, Stanford University School of Medicine, Stanford, CA 94305-5426.

number of different voltage-dependent ion channels, including voltage-dependent sodium channels (for reviews see Catterall, 1992; Stuhmer and Parekh, 1992), calcium channels (for review see Tsien, Ellinor, and Horne, 1991), and potassium channels (for reviews see Hoshi and Zagotta, 1993; Salkoff, Baker, Butler, Covarrubias, Pak, and Wei, 1992). Many of these channels share considerable sequence similarity. In particular, they possess a region of ~20 amino acids, the S4 segment, that contains a positively charged residue at every third amino acid with intervening hydrophobic residues (Noda, Shimizu, Tanabe, Takai, Kayano, Ikeda, Takahashi, Nakayama, Kanaoka, Minamino, Kahugawa, Matsuo, Raftery, Hirose, Inayama, Hayashida, Miyata, and Numa, 1984). This region has been proposed to span the membrane and represent the voltage sensor for the voltage-dependent transitions (Catterall, 1986; Durell and Guy, 1992; Greenblatt, Blatt, and Montal, 1985; Guy and Seetharamulu, 1986; Noda, Ikeda, Suzuki, Takeshima, Takahashi, Kuno, and Numa, 1986). In support of this idea, mutations of the S4 segment have been shown to alter the voltage sensitivity of a number of different channel types (Liman, Hess, Weaver, and Koren, 1991; Lopez, Jan, and Jan, 1991; Papazian, Timpe, Jan, and Jan, 1991; Schoppa, McCormack, Tanouye, and Sigworth, 1992; Stuhmer, Conti, Suzuki, Wang, Noda, Yahagi, Kubo, and Numa, 1989). However, mutations in other regions of the channel have also been shown to alter the voltage-dependent activation processes (Gautam and Tanouye, 1990; Lichtinghagen, Stocker, Wittka, Boheim, Stuhmer, Ferrus, and Pongs, 1990; McCormack, Tanouye, Iverson, Lin, Ramaswami, McCormack, Campanelli, Mathew, and Rudy, 1991; Zagotta and Aldrich, 1990a) suggesting that other regions are also involved directly or indirectly in the activation conformational changes.

The amino acid sequence of the voltage-dependent sodium and calcium channels contain four homologous domains, each containing six putative transmembrane segments, including one S4 segment. However, the amino acid sequence of most voltage-dependent potassium channels, such as the *Shaker* channel cloned from *Drosophila*, is only approximately one fourth as long and contains only a single S4 segment (Kamb, Tseng, and Tanouye, 1988; Pongs, Kecskemethy, Muller, Krah, Baumann, Kiltz, Canal, Llamazares, and Ferrus, 1988; Tempel, Papazian, Schwarz, Jan, and Jan, 1987). Therefore the potassium channel peptide is thought to represent only a subunit of a multimeric voltage-dependent potassium channel. However, mRNA coding for this subunit is sufficient to direct the expression of voltage-dependent potassium channels in *Xenopus* oocytes indicating that functional channels can be formed from homomultimers of *Shaker* subunits (Iverson, Tanouye, Lester, Davidson, and Rudy, 1988; Timpe, Jan, and Jan, 1988; Timpe, Schwarz, Tempel, Papazian, Jan, and Jan, 1988; Zagotta, Hoshi, and Aldrich, 1989). Based on its sequence similarity to voltage-dependent sodium and calcium channels, the *Shaker* potassium channel is thought to function as a tetramer of four *Shaker* subunits. In support of this idea, MacKinnon (1991) has shown that block by scorpion toxin of heteromultimeric *Shaker* potassium channels, formed by different proportions of toxin-sensitive and toxin-insensitive subunits, is consistent with a tetrameric structure. Furthermore, the block of the external pore by tetraethylammonium (TEA) has been shown to involve the coordination of TEA by all four subunits (Heginbotham and MacKinnon, 1992; Kavanaugh, Hurst, Yakel, Varnum, Adelman, and North, 1992;

Liman, Tytgat, and Hess, 1992). The presence of multiple similar, or identical, subunits in potassium channel proteins suggests a possible physical mechanism for the multiple conformational changes occurring during activation. Opening of the channel might require separate conformational changes to occur in some or all of the subunits. This type of mechanism is typified by the model of Hodgkin and Huxley (Hodgkin and Huxley, 1952) for the activation of squid voltage-dependent potassium channels that involved the movement of four independent and identical gating particles.

Since the model of Hodgkin and Huxley (Hodgkin and Huxley, 1952) a number of other models have been proposed for the activation mechanism in voltage-dependent potassium channels (e.g. Cole and Moore, 1960; Gilly and Armstrong, 1982; Greene and Jones, 1993; Koren, Liman, Logothetis, Nadal, and Hess, 1990; Perozo, Papazian, Stefani, and Bezanilla, 1992; Tytgat and Hess, 1992; White and Bezanilla, 1985; Young and Moore, 1981; Zagotta and Aldrich, 1990b). Previously, we have proposed a gating mechanism for *Shaker* channels where a voltage-independent inactivation process is coupled to voltage-dependent activation (Zagotta and Aldrich, 1990b). The activation process was modeled as a voltage-dependent conformational change in each of four subunits, followed by a final voltage-independent opening transition. This model was based on a single-channel analysis of the native *Shaker* channels in *Drosophila* myotubes. The final voltage-independent transition was proposed to account for the voltage-independent bursting behavior of the channels at depolarized voltages. However, in that study, the details of the activation mechanism were poorly determined for the following reasons: (a) The native *Shaker* channels undergo a rapid inactivation that masks the time course of the macroscopic activation or deactivation. (b) The myotubes express several other voltage-dependent potassium channels that are unaltered in *Shaker* mutants (Zagotta, Brainard, and Aldrich, 1988) which prevent an accurate determination of the macroscopic kinetics of the *Shaker* channels. (c) The channel densities were too small to record gating currents. (d) Patches containing single *Shaker* channels were rare. (e) The whole-cell and single-channel currents exhibited a rundown, probably caused by an absorbing slow inactivation process, such as C-type inactivation (Hoshi, Zagotta, and Aldrich, 1991). (f) The subunit composition of the native *Shaker* channel is unknown, and the myotubes may express a heterogeneous population of channels with different compositions of alternatively spliced variants from the *Shaker* locus.

Many of these problems are overcome by the study of *Shaker* channels expressed by RNA injection into *Xenopus* oocytes. Because the oocytes do not contain an appreciable level of endogenous voltage-dependent channels, virtually all of the ionic and gating current arises from *Shaker* channels. By varying the amount of RNA injected into the oocyte, we can record single-channel currents, macroscopic currents, and gating currents all in cell-free patches in the same preparation. Perhaps most importantly, we can alter the channel's primary structure to optimize its properties for the study of activation. The *Shaker* locus is alternatively spliced, so that many different variants of the *Shaker* protein are produced from the same gene (Kamb et al., 1988; Pongs et al., 1988; Schwarz, Tempel, Papazian, Jan, and Jan, 1988). We have chosen to study channels from the ShB variant which normally undergo a very rapid N-type inactivation process, mediated by the amino terminal domain, and a

very slow C-type inactivation (Hoshi et al., 1991). We have previously shown that a deletion near the amino terminus, ShB Δ 6-46, disrupts the rapid N-type inactivation process that is mediated by the amino terminal domain (Hoshi, Zagotta, and Aldrich, 1990; Zagotta, Hoshi, and Aldrich, 1990). Therefore, by modifying the channel structure, we can study the activation process in these channels in the relative absence of inactivation.

Our analysis of the activation gating mechanism will be divided into three parts. In this paper we utilize single-channel recording to analyze the conformational transitions near the open state. The analysis of the single-channel currents provides a direct estimate of the number of open and closed conformations entered after first opening and of the rate and voltage-dependence of the transitions between these conformations (for review see Colquhoun and Hawks, 1983). In addition we explore whether any of the closed conformations that the channel enters after first opening also occur in the process of activation, as expected for a model with a final voltage independent opening transition (Zagotta and Aldrich, 1990*b*). In the following paper (Zagotta, Hoshi, Dittman, and Aldrich, 1994) we utilize steady state and kinetic measurements of the ionic and gating currents to identify several general properties of the activation gating mechanism that must be accounted for by any kinetic model. Finally, in the third paper (Zagotta, Hoshi, and Aldrich, 1994) we will consider a number of specific models for the activation process that incorporate the known tetrameric subunit composition. This concludes with the presentation of a model that can account for virtually all of our observations.

MATERIALS AND METHODS

Channel Expression

A mutant *Shaker* potassium channel, ShB Δ 6-46, was expressed in *Xenopus* oocytes by injecting cRNA as described previously (Hoshi et al., 1990; Zagotta et al., 1989). Recordings were typically made 1 to 7 d after the injection.

Electrophysiology

Recordings from the expressed channels were made using the cell-free inside-out or outside-out configuration of the patch-clamp method (Hamill, Marty, Neher, Sakmann, and Sigworth, 1981) as described previously (Hoshi et al., 1990; Zagotta et al., 1989). Data were acquired and analyzed using a Digital Equipment Corp. LSI 11/73-based minicomputer system. The output of the patch-clamp amplifier was low-pass filtered through an eight-pole Bessel filter (Frequency Devices, Haverhill, MA) and digitized at the frequencies indicated. Experiments were carried out at 20°C.

Unitary currents were recorded using borosilicate pipettes (VWR micropipettes). Data were digitized at 20 kHz. Low-pass filter frequencies were adjusted according to the single channel amplitudes as indicated in the figure legends. The data were typically filtered at 1 to 1.8 kHz in the voltage range of 0 to +50 mV. Leak and capacitive currents were subtracted using the data sweeps with no opening as described previously (Hoshi and Aldrich, 1988*b*). Opening and closing transitions were detected using 50% of the single channel amplitude at a given voltage as the threshold criterion. Open and closed durations were measured from these idealized records. The number of channels present in a patch was determined by observing the maximum number of channels open simultaneously at voltages where the probability of the channel being open was high. Only the data from single-channel patches are presented.

Substates

Shaker potassium channels sometimes showed multiple conductance levels. The main conductance level was 9 to 10 pS in the range of -50 to 50 mV using the standard solutions (see below). Subconductance levels, ~ 60 and 30% of the amplitude of the full conductance state were also observed. The occurrences and the durations of these subconductance states were variable among the patches. Those sweeps with high substate occurrences were excluded from the idealization.

Duration Fitting

The open and closed durations were fitted with sums of exponential probability density functions (pdf's) using the maximum likelihood method with simplex optimization. The fit was corrected for the left censor time or the dead time of the recording system and for the right censor time or the limited pulse duration (Colquhoun and Sigworth, 1983; Hoshi and Aldrich, 1988a). The left censor time was estimated as $0.253/f$, where f represents the filter cut-off frequency in Hz. Open and closed duration histograms are shown using the log-binning transformation of Sine and Sigworth (Sigworth and Sine, 1987). Only those events longer than the left censor time are shown. The number of exponential components present in a data set was determined using the likelihood ratio test (Kalbfleisch, 1985). An additional component was included only when the probability of the data requiring one additional component was > 0.95 .

The first latency distributions were corrected for the filter delay time. The delay time was estimated as $0.506/f$, where f represents the filter cut-off frequency in Hz.

Correction for Missed Events

Values of the rate constants in the three-state kinetic models considered were estimated with corrections for those events too short to be resolved (Blatz and Magleby, 1986). This method involves calculation of the four effective rate constant values given the model considered and the left censor time (the dead time of the recording system). For each data set, the effective rate constant values were calculated by estimating the fraction of the total events longer than the left censor time. The rate constant values were optimized separately for the open and closed time parameters so that the time constant in the open time histogram and the time constants in the closed histogram predicted by the effective rate constants match the experimentally observed values.

Error Estimates

Errors associated with the estimation of the rate constants with corrections for missed events are estimated using the method of bootstrap or sampling with replacements, essentially the same as that of Horn (1987).

Solutions

The standard extracellular solution contained (in millimolar): 140 NaCl, 2 KCl, 6 MgCl₂, 5 HEPES (NaOH), pH 7.1. The cytoplasmic solution contained (in millimolar): 140 KCl, 11 EGTA, 2 MgCl₂, 1 CaCl₂, 10 HEPES (*N*-methylglucamine (NMG)), pH 7.2; free [Ca²⁺] is ~ 10 nM.

RESULTS

The gating of single *Shaker* potassium channels involves transitions among a number of distinct classes of open and closed states. After a short delay, voltage steps elicit a

short burst of openings followed by a relatively long duration closed event corresponding to the inactivated state of the channel (Zagotta et al., 1989). Inactivation produces a time-dependent decay in the probability that the channel is open and a decay in the macroscopic current flowing through a number of channels in response to a voltage step. Because the inactivation process in the ShB variant is quite rapid,

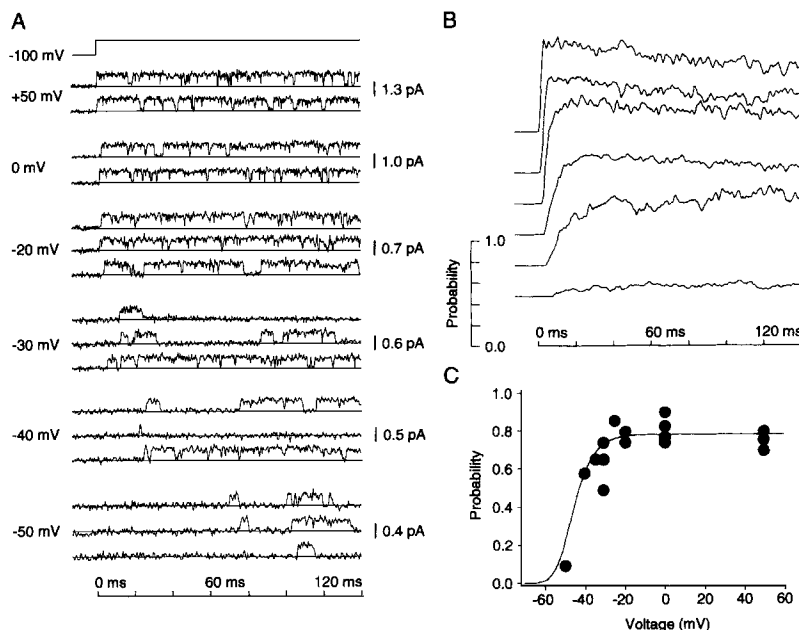


FIGURE 1. (A) Representative openings of ShB Δ 6-46 elicited in response to depolarizing voltage pulses. The data at +50, 0, -20, -30, -40, and -50 mV were filtered at 1.5, 1.2, 0.9, 0.8, 0.6, and 0.5 kHz, respectively. The voltage pulses were applied every 6 s. (B) Ensemble averages of the single-channel currents expressed as probabilities. 50–200 data sweeps were included in the averages. (C) Voltage dependence of the steady-state probability of the channel being open. Peak probabilities recorded from the ensemble averages are plotted against the voltage. Data from several patches are shown. The smooth curve represents the fourth power of a Boltzmann distribution expressed by the following equation:

$$P_0 = P_0^{\max} \left[\frac{1}{1 + e^{-(V - V_{1/2})zF/RT}} \right]^4$$

where P_0^{\max} is the maximum open probability (0.8); V is membrane voltage, $V_{1/2}$ is the voltage where the Boltzmann distribution is equal to 0.5 (-54 mV), z is the equivalent charge movement associated with the Boltzmann distribution (four electronic charges), F is Faraday's constant, R is the universal gas constant, and T is the absolute temperature.

the channel is given little chance to undergo other gating transitions before inactivating, making it difficult to study the transitions among other states of the channel. This inactivated conformation can be selectively removed from the ShB channel by mutations that delete part or all of the amino terminal domain (Hoshi et al., 1990) allowing a more detailed study of these other transitions. Fig. 1 A shows the

single-channel behavior of one of these mutant channels, ShB Δ 6-46, where amino acids 6 to 46 have been deleted from the channel protein. Like the wild-type channels, these channels also open after a delay in response to depolarizing steps to voltages above -50 mV. Furthermore, the latency to first opening becomes shorter as the voltage step becomes more depolarized. However, unlike wild-type channels, ShB Δ 6-46 channels generally continue to burst for the duration of these short pulses and do not enter a long duration closed state at depolarized voltages. While the rapid inactivation process has been removed, these channels are still able to undergo a second type of inactivation process, termed C-type inactivation, that is slow in ShB Δ 6-46 channels and is not appreciable on this time scale (Hoshi et al., 1991).

The average behavior of the channels can be seen in the ensemble averages shown in Fig. 1 B. The time course of the probability relaxation to steady state becomes more rapid as the voltage is increased from -50 to $+50$ mV. Moreover, the probability that the channel is open does not exhibit a time-dependent decay on this time scale, as expected after the removal of the fast inactivation process. Fig. 1 C plots the steady-state probability that the channel is open as a function of voltage. This probability increases steeply between -50 and -30 mV but saturates at about 0.8 above -30 mV. This voltage dependence is fitted with a fourth power of a Boltzmann distribution that also fits the voltage dependence of the conductance from macroscopic currents (see following paper, Zagotta et al., 1994). In the following discussion we will refer to voltages above -30 mV as "depolarized voltages," voltages between -60 and -30 mV as the "activation voltage range," and voltage below -60 mV as "hyperpolarized voltages." The exact dividing lines between these various ranges is somewhat arbitrary, so that when we refer to a property of the channel in a particular voltage range we mean only to indicate that it is most prominent in that range.

The Activation Time Course and Voltage Dependence at Depolarized Voltages are Determined by the Transitions Before First Opening

Most of the voltage dependence in the time course of the ensemble averages arises from a voltage dependence in the latencies to first opening. Fig. 2 A plots the cumulative distribution of first latencies for voltages between -50 and $+50$ mV. At depolarized voltages, these distributions are sigmoidal at the foot. This departure of the distribution from a single-exponential distribution is generally interpreted to indicate that the channel must progress through multiple closed states, or undergo multiple conformational transitions, before opening. The first latency distributions saturate near a probability of 1, indicating that only rarely did the voltage pulse fail to elicit openings and that the occurrence of C-type inactivation from closed states before channel opening is relatively rare under these experimental conditions. As in the ensemble averages, the time course of the first latency distributions becomes more rapid as the voltage becomes more depolarized. The activation and first-latency time courses are expected to be similar when the value of the leaving rate constant from the open state is negligible. These time courses would differ when the leaving rate is fast, as is the case for a channel undergoing rapid inactivation from the open state (Aldrich, Corey, and Stevens, 1983). The time courses of the ensemble averages and first latency distributions are compared in Fig. 2 B. In this figure, the saturating

amplitudes of the ensemble averages were scaled to that of the cumulative distributions of first latencies to directly compare their time courses. The similarities in these wave forms argues that the voltage-dependent kinetics of the macroscopic currents elicited by steps to depolarized voltages is largely determined from voltage dependence in the conformational transitions before the channel first opens and not from voltage-dependent transitions to other open or closed states populated after first opening.

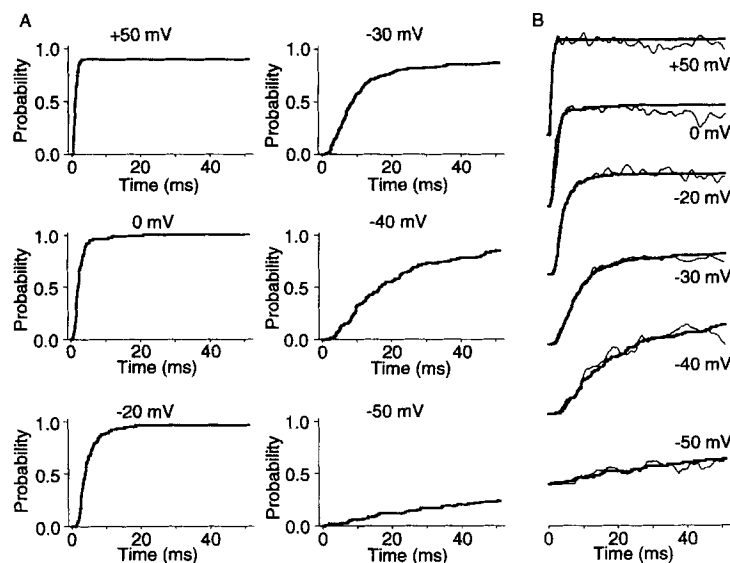


FIGURE 2. (A) Cumulative distributions of first latencies recorded at different voltages. The distributions show the probabilities that the channel first opened by the times indicated. The openings were elicited in response to 152 ms-depolarizing pulses from -100 mV. (B) Comparisons of the first latency distributions (*thick line*) and ensemble averages (*thin line*). The curves were scaled so that the steady-state levels coincide.

Transitions After First Opening Are Voltage-independent at Depolarized Voltages

The durations of the open and closed events elicited by steps to voltages between -50 and $+50$ mV were analyzed in terms of a time homogeneous Markov process. This analysis of the single-channel gating kinetics predicts that the distribution of closed durations will be described by a sum of N exponential components where N represents the minimum number of closed states that the channel enters after opening. The maximum likelihood that the measured closed durations at each voltage were described by a distribution of N exponential components was calculated by varying the time constant and amplitude of each component. The maximum likelihoods for 1 to 3 exponential components were then compared by the likelihood ratio test to determine the number of significant components required to describe the distribution of closed durations. This analysis of the closed durations reveals the occurrence of at least two distinct closed conformations after the channel first opens

at depolarized voltages and three closed conformations in the activation voltage range ($P < 0.05$).

Fig. 3 *A* plots the frequency distribution of closed events from a patch containing a single ShB Δ 6-46 channel during steps to voltages between -50 and $+50$ mV. The distributions are plotted and fitted with the maximum likelihood estimates of distributions containing two or three exponential components. The time constants and amplitudes of each component from a number of different single-channel patches are plotted as a function of voltage in Fig. 3 *B*. The fast component, ~ 0.3 ms in duration, can be seen as flicker closings in the single-channel records of Fig. 1 *A*. These closings represent the most frequently observed closed events, at least 90%,

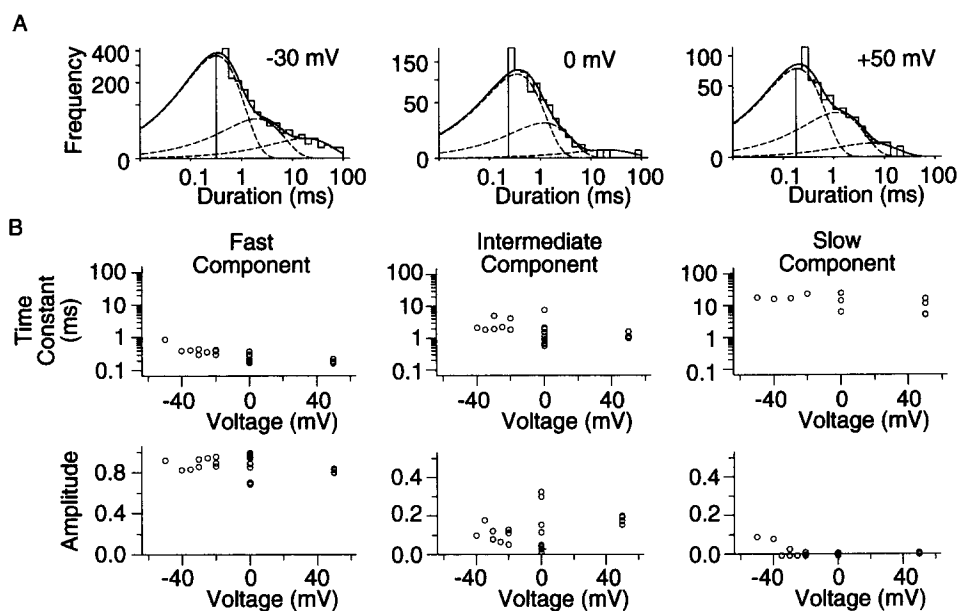


FIGURE 3. (*A*) Closed duration histograms measured at different voltages from ShB Δ 6-46. The data were fitted with a sum of three exponentials. The solid line represents the overall fitted curves and the dashed lines indicate the underlying individual components. (*B*) Voltage dependence of the time constants and relative amplitudes of the three exponential components.

which is an underestimate due to their observed numbers being limited by filter frequency. The duration and frequency of these events is only very weakly dependent on voltage between -50 and $+50$ mV, decreasing by about a factor of two over a 100 mV voltage range. In general, a one-to-one correspondence between a component of the closed time histogram and a discrete closed state can only be made when transitions between closed states do not occur. If the fast component arises primarily from a single closed conformation, this weak voltage-dependence suggests that there is little charge movement associated with the reopening conformational change, between the closed conformation and the transition state to opening.

The intermediate component of the distribution of closed durations is ~ 1.8 to 5 ms in duration and comprises $\sim 10\%$ of the closures. Its time constant and relative amplitude also display very little voltage dependence between -50 and $+50$ mV. Once again, if this component arises from a single closed conformation, this suggests that little charge movement occurs between the intermediate closed conformation and the transition state to reopening. In contrast to the fast and intermediate components, the slow component is frequently not significant at depolarized voltages and is more prevalent in the activation voltage range, at -40 mV and -50 mV, than at the depolarized voltages. These long closures, therefore, are likely to be partially due to channels that have returned to resting closed states from which they reopen

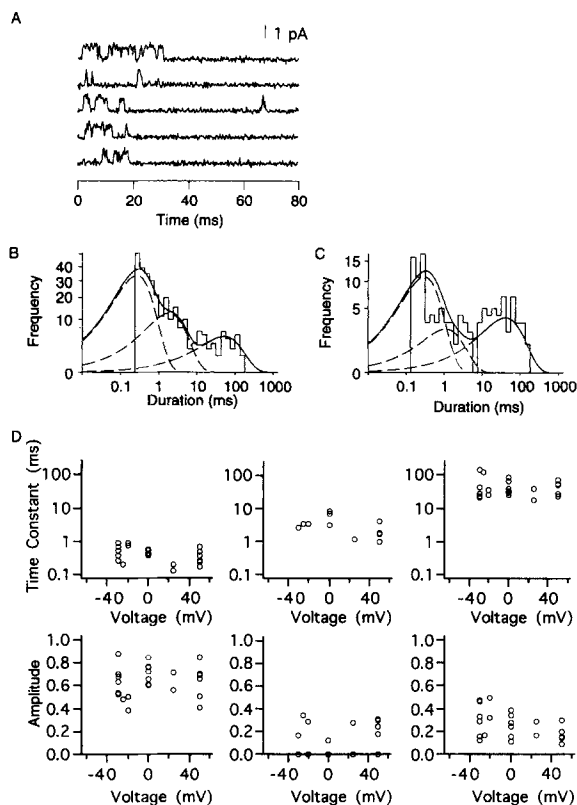


FIGURE 4. (A) Representative openings of a single ShD channel elicited in response to depolarizing voltage pulses from -100 to $+50$ mV. (B) Closed duration histogram from a ShD channel at $+50$ mV. The data were fitted with a sum of three exponential components with the solid line representing the overall fit curve and the dashed curves representing the individual components. (C) Closed duration histogram from a ShB channel at $+50$ mV. (D) Voltage dependence of the time constants and relative amplitudes of the three exponential components in the closed durations measured from ShD channels.

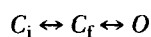
quite slowly. In addition the long closures could arise partially from C-type inactivation, particularly at depolarized voltages. Because this component is quite small and frequently not significant at depolarized voltages, we have ignored it for the following discussion.

In inactivating channels all of these closed durations are much less frequent due to rapid closures to a long-lived inactivated state shortly after opening. Nevertheless, the fast and intermediate components are present and not markedly altered in the closed time histograms from wild-type (inactivating) channels. Fig. 4A shows representative single channel records from a patch containing a single ShD channel in response to voltage steps to $+50$ mV. Frequency distributions of the closed durations

from patches containing a single ShB or ShD channel are shown in Figs. 4 *B* and *C*, respectively. These distributions are fitted with the maximum likelihood estimates of distributions containing three exponential components as discussed earlier. At depolarized voltages the closed events were significantly better described by a distribution containing three exponential components than by a distribution containing only two components ($P < 0.05$). For these wild-type channels, the slow component of the distribution of closed durations arises largely from sojourns in the N-type inactivated state. The fast and intermediate components, though, are still present and plotted as a function of voltage in Fig. 4 *D*. The short duration closures have also been observed in native *Shaker* channels (Zagotta and Aldrich, 1990*b*). The similarity of these components to their counterparts in ShBΔ6-46 channels suggests that neither class of closed duration is a residual form of the removed inactivation process and that neither requires inactivation or the amino terminal domain.

The closing conformational changes can be studied by an analysis of the open durations. In most patches the open events elicited by steps to voltages between -50 and $+50$ mV were sufficiently described by a single exponential distribution and did not warrant a distribution containing two components ($P < 0.05$). This suggests that only a single open conformation is kinetically distinguishable in the ShBΔ6-46 channel. Fig. 5 *A* plots the frequency distribution of open durations from a patch containing a single ShBΔ6-46 channel during steps to voltages between -50 and $+50$ mV. The distributions are fitted with the maximum likelihood estimate of a single exponential distribution. Fig. 5 *B* plots the maximum likelihood estimate of the time constant, from a number of different single-channel patches, as a function of voltage. As noted originally over a more limited voltage range in inactivating channels (Zagotta and Aldrich, 1990*b*; Zagotta et al., 1989), the mean open duration has very little voltage dependence between -50 and 50 mV. In fact, the small trend for the measured open durations to decrease with increasing voltage is eliminated when these data are analyzed correcting for missed events (see below). The open duration is governed by the rate constants of all of the closing conformational changes and is numerically equal to the reciprocal of the sum of all the closing rate constants. This sum is dominated by the most rapid, and therefore most frequent, closing rate constant. Since the flicker closings are the most frequent closed events at depolarized voltages, this voltage independence of the open times indicates that there is little charge movement associated with the closing conformational change producing these flickers.

The above analysis has indicated that, after opening at depolarized voltages, the channel can sojourn in at least one open conformation and two distinct closed conformations. Therefore a kinetic scheme containing only three states is sufficient to describe the gating behavior under these conditions. This is a subset of the overall kinetic scheme and consists only of states that the channel enters after opening at depolarized voltages. The distributions of the open and closed durations display very little voltage dependence at depolarized voltages, indicating that the rates of the various conformational changes are not voltage dependent. We have considered the two possible noncyclic three-state kinetic models to account for the single-channel behavior at depolarized voltages:



SCHEME I

and



SCHEME II

where C_i represents a closed state with intermediate dwell time, C_f represents a closed state with short dwell time, and O represents the open conformation. We have not considered the cyclic scheme where transitions are allowed between all three states. The cyclic scheme contains too many free parameters for the unique

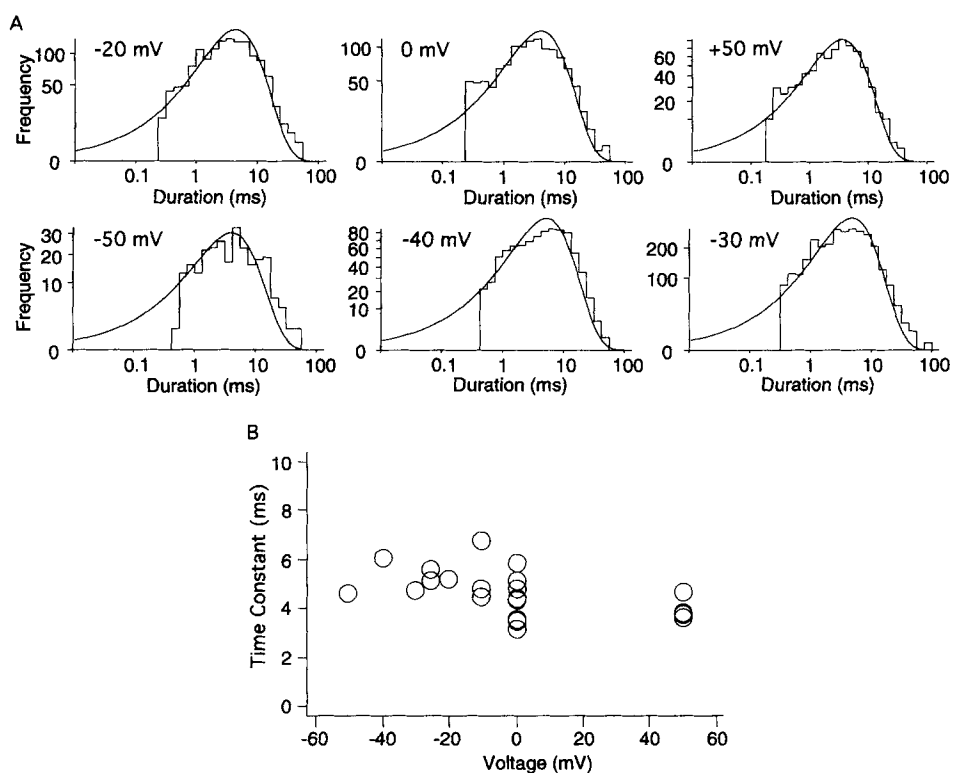


FIGURE 5. (A) Open duration histograms at different voltages from ShBA6-46. Each data set was fitted with a single exponential probability density function (*smooth line*). The openings were elicited as in Fig. 1. (B) Voltage dependence of the time constants of the open durations.

determination of its transition rate constants. In Scheme I, the channel, after activating, can open and close by only a single pathway, while in Scheme II there are two pathways for opening and closing. This distinction creates a very different interpretation of the time constants describing the open and closed time distributions. For Scheme I, the reciprocal of the mean open time is a direct measure of the rate of the closing conformational change while in Scheme II it equals the sum of the rate constants for two different closing conformational changes. An even larger difference exists in interpreting the time constants of the closed time distribution.

For Scheme II, the reciprocals of the two time constants are a measure of the two reopening rate constants. However, for Scheme I, both time constants are a function of several rate constants in the model and therefore cannot be directly interpreted in terms of the rate of any single conformational change.

With only the steady-state measurements of open and closed durations, it is impossible to discriminate between these schemes since both produce exactly equivalent fits to the open and closed time distributions. The four rate constants in each model are completely determined by four parameters from the steady state measurements of open and closed durations: the time constant from the distribution

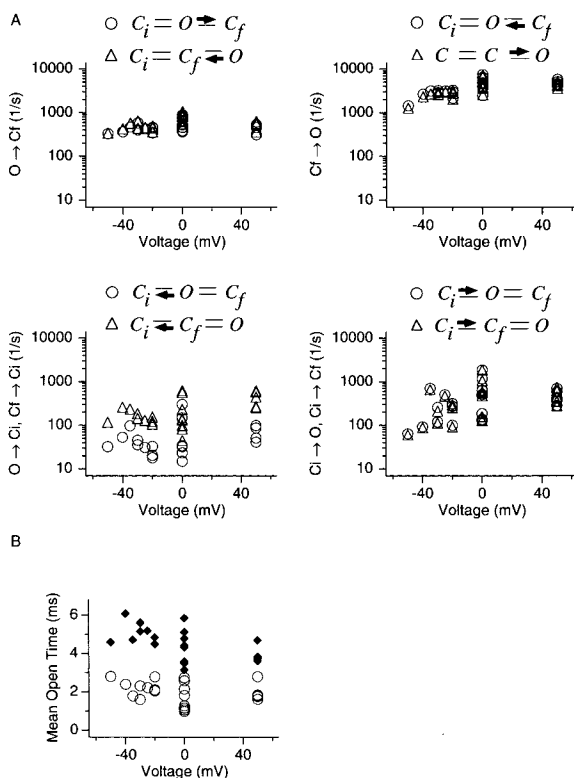


FIGURE 6. (A) Rate constants estimated for Scheme I: $C_i \leftrightarrow C_f \leftrightarrow O$ (Δ); and Scheme II: $C_i \leftrightarrow O \leftrightarrow C_f$ (\circ) with corrections for missed events. (B) Voltage dependence of the measured mean open duration (\blacklozenge) and of that predicted by Scheme II: $C_i \leftrightarrow O \leftrightarrow C_f$ (\circ).

of open durations, the two time constants from the distribution of closed durations, and the relative amplitude of the two components in the closed durations. The rate constants for each model were calculated for voltages between -50 and $+50$ mV, as outlined in the methods section, using the parameters from the maximum likelihood fits and are plotted as a function of voltage for several experiments in Fig. 6 A. Using the procedure of Blatz and Magleby (Blatz and Magleby, 1986), these rate constants were corrected for missed opening and closing events that were too rapid and therefore did not reach the half amplitude criterion. As expected, all four rate constants in each model are nearly voltage-independent, particularly at depolarized

voltages (≥ -30 mV). The average rate constants pooled from a number of experiments between -30 and 50 mV are presented in Table I. The two models predict very similar rate constants for entry and exit from the Cf state and rate constants for exit from the Ci state. Transitions into the Cf state are ~ 10 times more frequent than transitions into the Ci state, and the average dwell time in the Cf state (~ 260 μ s) is ~ 10 times shorter than the dwell time in the Ci state (~ 2.6 ms). The major difference in the rate constants between the two models lies in the rate constant for entry into the Ci state which is approximately five times larger for Scheme I than for Scheme II to counteract the very rapid reopening transition $Cf \rightarrow O$ in Scheme I.

The missed events corrections had the largest effect on the measured open durations. Fig. 6B plots the predicted open durations for the two models (*open symbols*) and the measured open durations (*closed symbols*) as a function of voltage. Because many of the predicted short closing events were not detected, the measured open durations were artificially long, especially at the more hyperpolarized voltages

TABLE I
Summary of the Rate Constants for Schemes II (VII) and III (VIII)

Transition	Scheme II (VII) rate constant s^{-1}	Scheme III (VIII) rate constant s^{-1}
O \rightarrow Cf	$550 \pm 68^*$	460 ± 47
Cf \rightarrow O	$3,600 \pm 570$	$3,800 \pm 570$
Cf \rightarrow Ci or O \rightarrow Ci	154 ± 51	34 ± 10
Ci \rightarrow Cf or Ci \rightarrow O	350 ± 150	360 ± 150
... C \leftarrow O	$13.5 e^{-V/22}$	$13.5 e^{-V/22}$

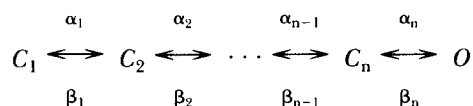
*These numbers are means \pm the 95% confidence intervals of the medians.

$^{\dagger}V$ is the membrane voltage in millivolts.

where generally the data were more heavily filtered. After this correction, the small amount of apparent voltage-dependence in the distributions of open durations between -50 and $+50$ mV is virtually eliminated, and the rate constants for the closing transitions in each model were voltage independent.

The Ci State Is Not Traversed During Channel Activation

The voltage-dependent activation of the channels involves a number of transitions among closed states before opening. This is evidenced by the sigmoidal time course of the macroscopic activation and the first latency cumulative distributions shown in Fig. 2, and can be summarized by the linear scheme for activation shown below:



SCHEME III

where α_1 to α_n represent the rate constants of the forward transitions and β_1 to β_n represent the rate constants of the reverse transitions and n is the number of closed states. The number of closed states in the activation pathway and their properties are

discussed in detail in the following paper (Zagotta et al., 1994). The above analysis has indicated that once open, the channel can enter at least two closed states at depolarized voltages. In the following analysis, we examine whether the closed states that the channel enters after opening might constitute any of the closed states in the activation pathway of Scheme III. Stated another way, which closed states that the channel enters after opening must be also traversed before opening?

At depolarized voltages, the distributions of closed durations exhibit two exponential components indicating the occurrence of at least two closed states after opening. If both of these closed states are also traversed before opening, then the first latency distribution will also include these two exponential components, though with different relative amplitudes. Furthermore, if the channel must enter both of these closed states in the process of activation, then the cumulative distributions of first latencies must be less than or equal to that of the closed durations at all times. This can be illustrated by considering the linear model for activation in Scheme III. The cumulative distribution of first latencies represents the probability that the channel has first opened by time t , while the cumulative distribution of closed durations

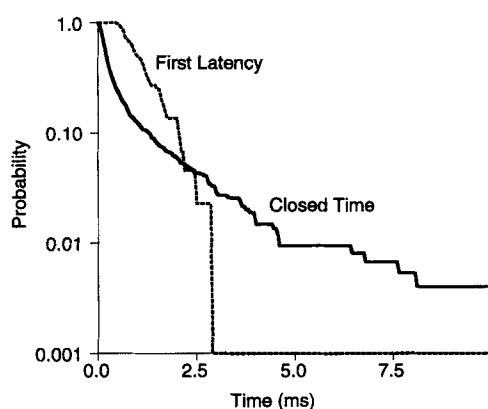


FIGURE 7. Comparison of the distributions of first latencies (*dashed line*) and closed durations (*solid line*) at +50 mV. The data are shown as complements of cumulative distributions, showing the probabilities that the durations are greater than the times indicated on the axis. The openings were elicited as in Fig. 1.

represents the probability that the channel has reopened by time t . For Scheme III, these distributions can be calculated as simply the time course of the probability of being open assuming that the open state is absorbing, that is β_n is zero. The cumulative distributions of first latencies are calculated with the initial condition that the channels are in state C_1 at time zero, while the distributions of closed times after first opening are calculated with the initial condition that the channels are in state C_n at time zero. Because at no time will the “have opened” probability be greater when the channels start in C_1 than when they start in C_n , the cumulative distribution of first latencies will always be less than that of the closed durations for Scheme III. Similarly the complement of the cumulative distribution, representing the probability of having not yet opened by the time on the abscissa, will always be greater for the first latencies than the closed durations if all of the closed durations are from states in the activation pathway, as in Scheme III.

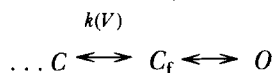
The complement of the cumulative distributions of first latencies and closed times with voltage steps to +50 mV are compared in Fig. 7. While at short times the first latency distribution is greater than the closed time distribution, the distributions

eventually cross so that the probability that the channel has not reopened by time t after closing is greater than the probability that the channel has not opened for the first time by time t after a voltage step. This crossing of the distributions was consistently observed and indicates that, after first opening, the channel often undergoes sojourns in one or more closed states that are not always traversed in the process of activation. Therefore, after opening, the channel must enter a closed state that only occurs after opening, or a closed state that exists as a branch off of the main activation pathway and occurs only infrequently before opening.

The crossing of the distributions occurs because the intermediate component of the distribution of closed durations is quite prominent in the closed durations at +50 mV and is notably longer than the median first latency at +50 mV. If the closed state(s) producing this component were in the activation pathway, the first latency could never be faster than the time required for half of the channels to exit that state(s). This can best be seen in the analysis of the single-channel behavior at depolarized voltages shown in Fig. 6 and Table I. For both Schemes I and II, the rate constant for exit from the C_i state is $<400 \text{ s}^{-1}$. Therefore, if the C_i state were in the activation pathway, the median first latencies could not be less than 1.7 ms, the time required for half of the channels to exit the C_i state. Because the median first latency is about 1.1 ms at +50 mV (range 0.9 to 1.5 ms), the C_i state cannot always be traversed during activation. This conclusion means that the C_i state is either not in the activation pathway or is on a branch where it is not obligatory for activation, as would exist in a cyclic scheme.

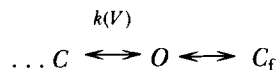
The C_f State Is Not Traversed During Channel Deactivation

For both Schemes I and II, the rate of exit from the C_f state is quite rapid compared to the overall time course of activation. This leaves open the possibility that the C_f closed state is in the activation pathway. As proposed by Zagotta and Aldrich (Zagotta and Aldrich, 1990b) for native *Shaker* channels, the C_f state might represent the last closed state in the activation pathway, as summarized in the scheme below:



SCHEME IV

where $\dots C$ represents other closed states in the activation pathway. In this model, and Scheme V below, the intermediate closed state C_i has been omitted for clarity. Because the first latencies become shorter as the voltage is depolarized, the rate constants associated with the activation pathway are shown as voltage-dependent. However, as shown earlier, the rates of the transitions between the open state and the C_f state are nearly voltage independent, at least at depolarized voltages. Therefore, this model would postulate a final voltage-independent transition for the activation process. Alternatively, the C_f state might not be in the activation pathway, as summarized in the scheme below:



SCHEME V

In this model, the channel can only enter the Cf state after opening. As in the case with Schemes I and II, these two models cannot be distinguished based on steady state single-channel data at any given voltage. However, they might be expected to differ in their predictions for the voltage dependence of the open durations. In Scheme IV, the channel exhibits only one type of closing transition, which has a rate that is voltage-independent at depolarized voltages. Therefore, if the $O \rightarrow Cf$ transition rate remains voltage-independent at more hyperpolarized voltages, the open durations will remain voltage-independent. Alternatively, in Scheme V, the channel exhibits two types of closing transitions. At depolarized voltages the channel closes primarily to Cf, producing voltage-independent open durations. However, at hyperpolarized voltages, the voltage-dependent closing rate to the activation pathway, $\dots C \leftarrow O$, might become appreciable, producing shorter closing durations. Therefore this model would predict open durations that decrease at hyperpolarized voltages.

To examine more closely the voltage dependence of the closing transitions, we have analyzed the closing kinetics of single ShBA6-46 channels during deactivation at hyperpolarized voltages after being opened by a depolarizing voltage step. To overcome the problem that, in normal solutions, the single-channel currents are exceedingly small at these hyperpolarized voltages, we have recorded the inward single-channel currents with 140 mM K^+ in the external solution.

In the following paper (Zagotta et al., 1994), we will show that some external monovalent cations alter the rate of macroscopic deactivation. However unlike in some other potassium channels (Armstrong, 1981; Cahalan, Chandy, DeCoursey, and Gupta, 1985; Matteson and Swenson, 1986), 140 mM external K^+ appeared to have very little effect on the time course and voltage dependence of macroscopic deactivation at hyperpolarized voltages. Furthermore, below we show that 140 mM external K^+ does not significantly alter the open durations in the activation and depolarized voltage ranges. Therefore, it is likely that high external K^+ does not markedly alter the closing transitions in *Shaker* channels. A similar observation has been made for the type L potassium channel from lymphocytes (Shapiro and DeCoursey, 1991). Fig. 8A shows representative single-channel behavior during voltage steps to -90 mV (*left*) or -60 mV (*right*) after a step to $+50$ mV. Upon hyperpolarization, these channels elicit a short burst of openings before entering an absorbing closed conformation. The burst durations were significantly shorter at -90 mV than at -60 mV as indicated by the ensemble average in Fig. 8B. The average probability of being open decays much more rapidly at -90 mV than at -60 mV.

The number of kinetically distinguishable closed conformations that the channel enters during the bursts was examined by an analysis of the closed durations at -90 and -60 mV, omitting the final long closed events that were censored by the termination of the pulse. The closed events elicited by repolarizations to -60 mV were significantly better described by a distribution containing three exponential components than by a distribution containing only 2 components ($P < 0.05$). The closed events at -90 mV were sufficiently described by a single exponential distribution and did not warrant a distribution containing two components ($P < 0.05$). Fig. 9 plots the frequency distribution of closed events from a patch containing a single channel during repolarizing voltage steps to -90 or -60 mV together with the maximum likelihood estimates of distributions containing one and

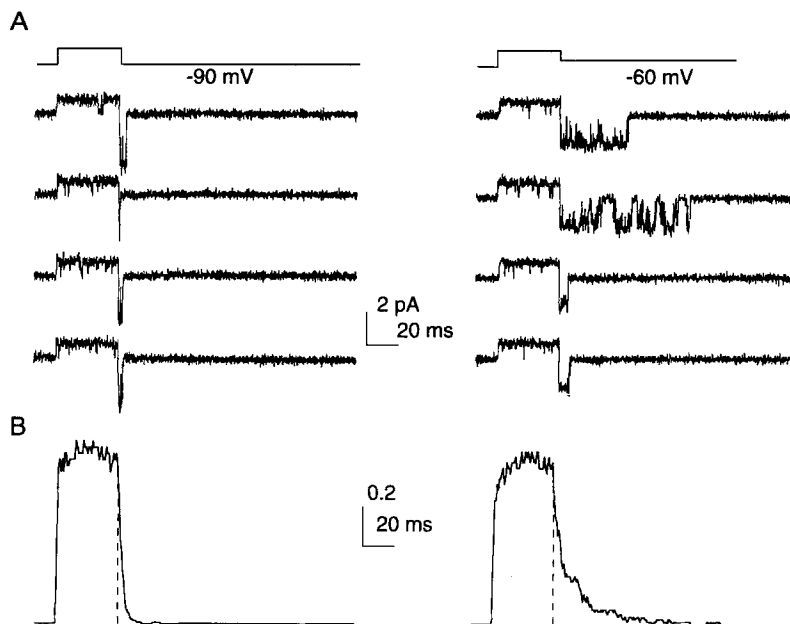


FIGURE 8. (A) Single-channel currents recorded in the high K^+ solution. The extracellular solution contained (in millimolar): 140 KCl, 6 $MgCl_2$, 5 HEPES (NaOH), pH 7.1. The openings were elicited in response to depolarizing pulses to +50 mV for 40 ms and then to -90 mV (*left*) or -60 mV (*right*). The data were filtered at 1.7 kHz (-90 mV) and 1.5 kHz (-60 mV). (B) Ensemble averages expressed as probabilities.

three exponential components respectively. Both distributions contain a rapid component with a time constant between 0.2 and 0.4 ms, similar to the rapid component of the closed time distributions between -50 and +50 mV in normal solutions (See Fig. 3). In addition, the distribution at -60 mV contains a component with a time constant of 1.1 ms, similar to the intermediate component seen at more depolarized voltages. At -60 mV, the distribution of closed durations also displayed a very slow component (~ 28 ms). The histogram contains very few of these long

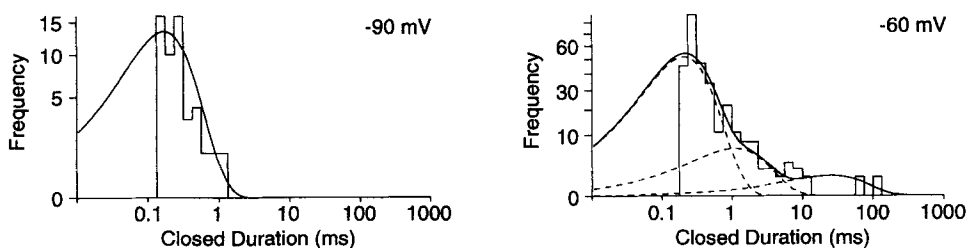


FIGURE 9. Frequency histograms of the closed durations recorded at -90 mV (*left*) and at -60 mV (*right*) after 40 ms-pulses to +50 mV. The durations at -90 mV were fitted with a single exponential with a time constant of 0.2 ms. The durations at -60 mV were fitted with a sum of three exponentials with time constants of 0.25, 1.1, and 28 ms. Their respective amplitudes were 0.88, 0.11, and 0.01.

duration closures at -60 mV because most of the events were censored by the end of the pulse and omitted. Consequently an accurate measure of this component of the closed duration distribution was impossible with these limited pulse durations. At -90 mV the channel entered a long closure in <2 ms and almost never returned to the open state for the remainder of hyperpolarizing pulse (80 ms). This indicates that the conformation(s) producing these long duration closures is very energetically stable relative to the open state at hyperpolarized voltages, as expected if it constitutes a closed state(s) in the activation pathway. Therefore, this analysis of the closed durations is consistent with a model where the channel undergoes transitions among C_f and C_i before entering $\dots C$ at -60 mV but rapidly enters $\dots C$ at -90 mV.

This voltage-dependent burst duration might be explained by either Schemes IV or V with a voltage-dependent rate for the transition into the states designated $\dots C$. However, if the $O \rightarrow C_f$ rate constant remains voltage independent at hyperpolarized voltages, then Scheme IV predicts that the open durations will be voltage-independent while Scheme V predicts that the open durations will decrease with increasing hyperpolarization. We therefore analyzed the open durations during deactivation at these hyperpolarized voltages. As at depolarized voltages, a maximum likelihood analysis indicated that open events elicited by steps to voltages between -100 and -50 mV were sufficiently described by a single exponential distribution and did not warrant a distribution containing two components ($P < 0.05$). This indicated that there is still only one kinetically distinguishable open conformation at hyperpolarized voltages. Fig. 10A plots the frequency distribution of open durations from a patch containing a single channel during voltage steps to -90 or -60 mV after a step to $+50$ mV. The distributions are fitted with the maximum likelihood estimate of a single exponential distribution.

Fig. 10B plots the maximum likelihood estimate of the time constant of the distribution describing the open durations, τ_o , as a function of voltage from both channels recorded in normal solutions (*circles*) and in 140 mM external K^+ (*triangles*). The open durations at -40 mV in 140 mM K^+ tend to be somewhat less than those in normal solutions due to missed closed events caused by the greater filtering in normal solutions. After correction for missed events the open durations in normal solutions are similar to those in 140 mM K^+ (see Fig. 6). In 140 mM K^+ , the open durations are also unaltered between -40 and $+50$ mV, indicating a voltage-independent closing transition at depolarized voltage, as in normal solutions. However, the mean open duration decreased from about 3 ms at -40 mV to 2 ms at -60 mV, and to 1 ms at -90 mV, indicating that there must be a voltage-dependent closing transition at these hyperpolarized voltages. $1/\tau_o$ is a direct measure of the rate constant for the transition $O \rightarrow C_f$ in Scheme IV, which contains only one closing transition. As shown in Fig. 11A, $1/\tau_o$ decreases exponentially with voltage at hyperpolarized voltages but saturates at a nonzero value at depolarized voltages. The saturating closing rate at depolarized voltages is almost entirely due to closures to the C_f state and is much too fast to be accounted for by closures to the C_i state (not explicitly shown in Schemes IV and V). The saturating value is not an artifact of missed closing events, as missed closings would lead to an even higher saturating value. The presence of a saturating value departs from the expectations of a simple

exponential voltage dependence for the rate of a single transition involving the movement of charge or reorientation of a dipole between the open state and the transition state to closing (Stevens, 1978).

Scheme V, however, contains two closing transitions and therefore provides an explanation for the voltage dependence of the open durations that does not require nonexponential voltage dependence of individual rate constants. At depolarized voltages the channel closes primarily to Cf, producing voltage-independent open durations. However, at hyperpolarized voltages, the voltage-dependent closing rate

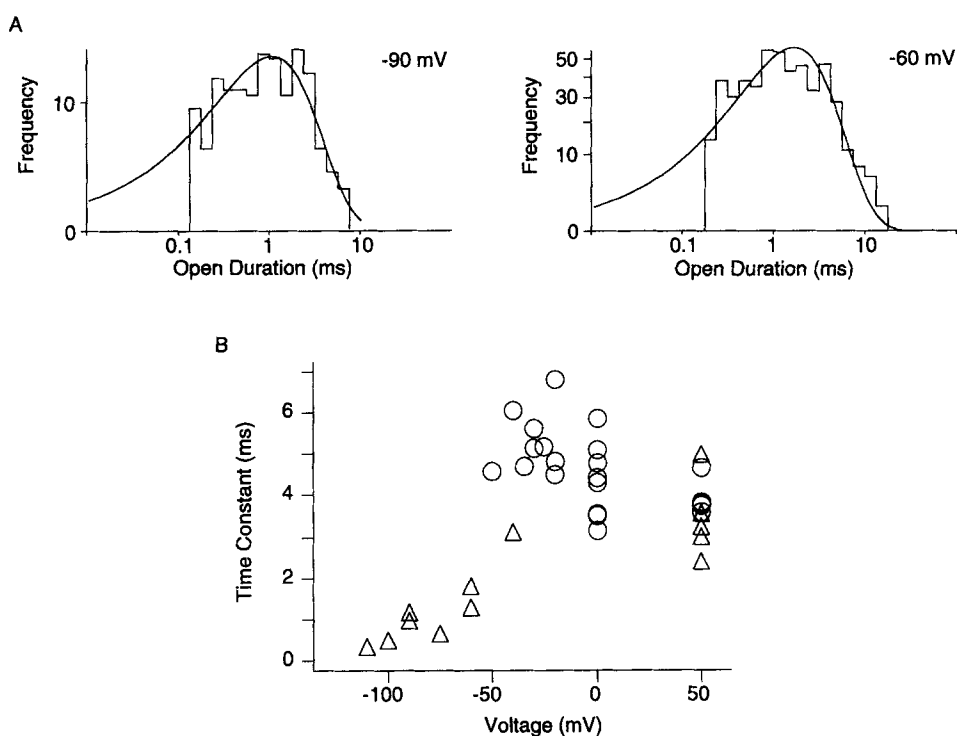


FIGURE 10. (A) Frequency histograms of the open durations measured at -90 mV (left) and -60 mV (right). The data at -90 mV and -60 mV were fitted with single exponentials with time constants of 1.1 ms and 1.6 ms, respectively (smooth lines). (B) Voltage dependence of the time constants of the open durations measured with the standard solutions (O) and with the high K^+ solution (Δ).

to the activation pathway, . . . $C \leftarrow O$, might become appreciable, producing shorter open durations. The total closing rate in Fig. 11 A would then represent the sum of two rate constants, a voltage independent $O \rightarrow Cf$ rate constant and an exponentially voltage dependent . . . $C \leftarrow O$ rate constant. For this reason, the voltage dependence of the total closing rate in Fig. 11 A was fit with the following equation:

$$1/\tau_o = k_c + k_0 e^{V/V_k} \quad (1)$$

where k_c is the value of the voltage-independent rate constant, k_0 is the value of the

voltage-dependent rate constant at 0 mV and V_k is the voltage dependence. The value of k_c , 400/s, is very similar to the $O \rightarrow Cf$ rate constant of Scheme I at depolarized voltages (Fig. 6). Note that if the channel can close directly to the Ci state, as in Scheme II, then k_c will also include a small contribution from the $O \rightarrow Ci$ rate. The $k_0 e^{V/V_k}$ term in Eq. 1 would represent the rate for the $\dots C \leftarrow O$ transition in Scheme V. Note that the rate constant for this transition at 0 mV (13.5/s) is very small so that the channel only rarely closes to the deactivation pathway at these depolarized voltages. The voltage-dependence of the rate constant (e-fold per 22 mV) corresponds to an equivalent charge movement of 1.16 electronic charges between the open state and the transition state to closing.

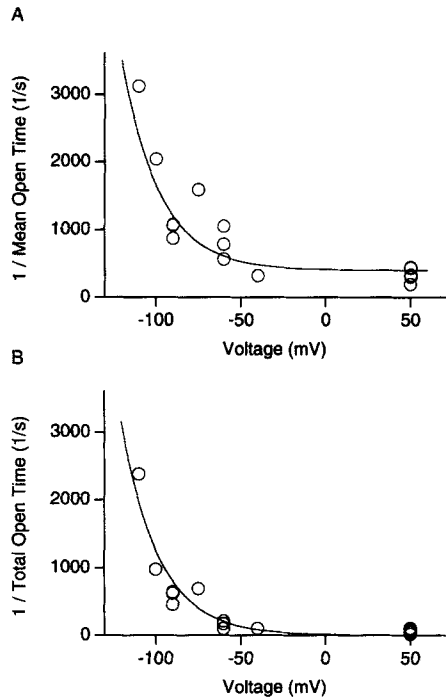
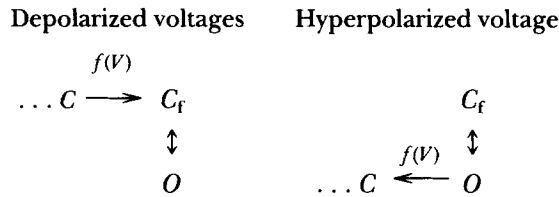


FIGURE 11. (A) Voltage dependence of the reciprocal of the mean open time. Reciprocal of the mean open durations obtained in the high K^+ solution were fitted with Eq. 1: $1/\tau_o = k_c + k_0 e^{V/V_k}$ (see Scheme V), where $k_c = 400/s$, $k_0 = 13.5/s$ and $V_k = 22$ mV. (B) Voltage dependence of the total open time (τ_{Bo}) in a burst. Burst analysis was performed using 10 ms as the criterion and the total open time is defined as the sum of all the open durations within a given burst. The data were fitted with Eq. 2, $1/\tau_{Bo} = k_0 e^{V/V_k}$. The values of k_0 and V_k are the same as in (A).

This analysis of the open durations has suggested that the Cf state is not in the pathway for deactivating from the open state and is therefore not in the activation pathway. The voltage dependence of the open durations might also be explained by a third model, summarized below:



SCHEME VI

This model represents a composite of Schemes IV and V. At depolarized voltages the channel enters the *C_f* state in the process of opening. However, at hyperpolarized voltages the channel closes directly to the . . . *C* state(s). Therefore the *C_f* state is in the activation pathway but not in the deactivation pathway. While at this time we cannot discriminate between Schemes V and VI, Scheme V has fewer transitions and therefore represents the more parsimonious model to account for the voltage dependence of the open durations. Together with the finding that the channel cannot always enter the *C_i* state before opening, this analysis suggests that neither of the closed states that the channel enters at depolarized voltages are in the activation pathway.

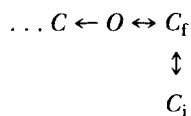
The rate for the . . . *C* ← *O* transition can be more directly measured by the distribution of the total time spent open during a burst. Bursts were defined as clusters of openings separated by closures < 10 ms in duration and terminated by closures greater than 10 ms in duration. The durations of the short and intermediate components of the distribution of closed durations are ~0.3 and 2 ms, respectively, while the duration of the slow component at hyperpolarized voltages, thought to arise from transition in the activation pathway, is ~20 to 50 ms. Therefore, the bursts should include transitions among the *O*, *C_f*, and *C_i* states and be terminated by transitions to the activation pathway. Furthermore, because we have suggested that the channel deactivates primarily from the open state, the reciprocal of the average total open time during the burst, $1/\tau_{Bo}$, is equal to the . . . *C* ← *O* rate constant. As shown in Fig. 11 *B*, $1/\tau_{Bo}$ decreases exponentially with voltage at hyperpolarized voltages and becomes very slow at depolarized voltages. The data were fitted with the following exponential equation:

$$1/\tau_{Bo} = k_0 e^{V/V_k} \quad (2)$$

where k_0 is the value of the voltage-dependent portion of the rate at 0 mV and V_k is the voltage dependence. The same values of k_0 and V_k used to fit the reciprocal of the open duration in Fig. 11 *A* also fit the reciprocal of the total open time during a burst in Fig. 11 *B*. This relationship is consistent with Scheme V where the same transition . . . *C* ← *O* both closes the channel and terminates the burst. This relationship would not necessarily hold for Scheme IV where the transition that closes the channel *O* → *C_f* is different from the transition that terminates the burst . . . *C* ← *C_f*.

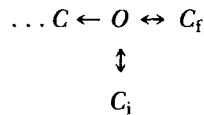
DISCUSSION

In the above analysis we have argued that the channel, once open, enters at least two different closed states at depolarized voltages and that neither of these closed states are obligatorily traversed during activation. The rates of the transitions among these closed states and the open state were nearly voltage-independent. Furthermore we have suggested that at hyperpolarized voltages the channel undergoes a voltage-dependent transition from the open state directly to a closed state in the activation pathway. These criteria can be met by two types of models, summarized below:



SCHEME VII

and



SCHEME VIII

At depolarized voltages the rate of the transition $\dots C \leftarrow O$ is virtually zero, and the channel bursts among the states O , C_f , and C_i . Schemes VII and VIII are then reduced to Schemes I and II respectively. However, at hyperpolarized voltages the bursting behavior is terminated by a transition into the activation closed states, $\dots C$. Just as we could not discriminate between Schemes I and II earlier, we also cannot discriminate between Schemes VII and VIII.

Table I shows a summary of the rate constants and their voltage-dependence for each of the transitions in Schemes VII and VIII. The rate constants for the voltage-independent transitions were determined from the median values from 19 experiments recorded in 2 mM external K^+ . The error estimates are the 95% confidence intervals of the medians. The rate and voltage dependence of the closing transition to the activation pathway were determined from the fits to the open time data in Fig. 11, recorded in 140 mM external K^+ . The variability in these estimates contains a contribution from two major sources: (a) errors due to fitting a limited number of single-channel events, and (b) variability between channels from different patches. To estimate the errors in fitting we have repeatedly resampled the single-channel events from selected experiments and performed the fitting procedures and rate constant calculations for each resampled data set. Fig. 12 shows boxplots of the rate constants for Scheme II calculated from all of the experiments, and boxplots of the rate constants calculated from 19 resamplings of the events from a typical experiment. Note that, in general, the rate constants from different experiments had a greater variability than the rate constants calculated from resampling the same experiment. This suggests that the errors introduced by fitting a limited number of events were smaller than the inherent variability between patches. This variability might be caused by either intrinsic differences in the channels or their environment, such as the surrounding lipid or their phosphorylation state, or by variation in the experimental conditions under which they were recorded, such as in the filter settings.

The occurrence of voltage-independent transitions among closed states after opening will have several effects on the measurements made from macroscopic currents. Perhaps the most obvious effect is that the peak open probability saturates at a value somewhat less than one (~ 0.8). This is important for estimating the number of channels in a patch from measurements of the macroscopic current. Furthermore, because 20% of the time the channels are not in the open state at the end of short depolarizing voltage steps, the macroscopic deactivation time course will reflect more than simply the rate of the closing transition to the activation pathway. In general, even if reopening from the activation pathway is negligible, the deactivation would be expected to have a triple exponential time course. This is because the relaxations of a system of n states ($\dots C$, O , C_f , and C_i) will contain $n-1$ characteristic time constants. In general, each time constant depends on the rate constants of all of

the transitions in the model. However, the C_f state produces a rapid time constant, generally too fast to directly observe ($\sim 230 \mu\text{s}$ for Scheme VIII). In the third paper of this series (Zagotta et al., 1994) we will show evidence for a small rapid phase in the tail currents, suggesting the occurrence of this fast exponential component.

The other two characteristic time constants of both Schemes VII and VIII are slow enough to be detected at voltages between -100 and -60 mV. For Scheme VIII, one time constant increases from 0.9 to 2.4 ms and the other increases from 2.9 to 6.5 ms between -100 and -60 mV. For deactivation, the exponential with the faster time constant is dominant at -100 mV and the exponential with the slower time constant is dominant at -60 mV. In the following paper (Zagotta et al., 1994), we will show that the time course of the tail currents can be approximated by a single-exponential

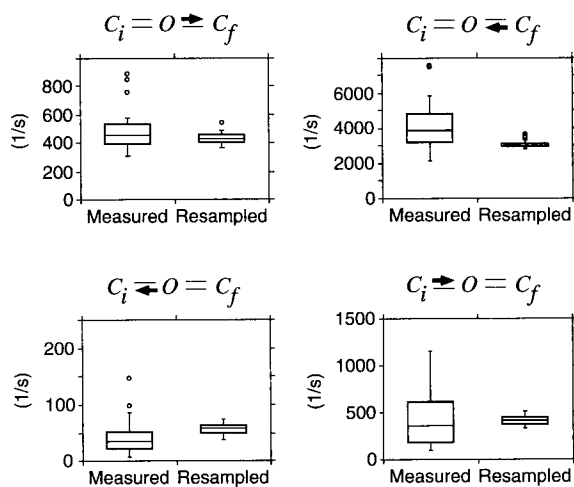


FIGURE 12. Variance associated with estimated parameters in Scheme II. The sampling variance was estimated by the method of sampling with replacements essentially the same as that of Horn (Horn, 1987). Open and closed durations were sampled from the data sets from a typical experiment for m and n times, where m and n represent the mean number of open and closed durations longer than the deadtime in the experiment. These durations were then used to estimate the parameters in Scheme

II with corrections for missed events in the same way that the original data sets were analyzed. Typically, each data set contained $\sim 1,000$ events. The data are shown using box plots (Tukey, 1977). The middle box covers the data between the 25th and 75th percentiles. The whiskers extending from the top and bottom of the box represent the main body of the data and circles represent outliers. For each rate constant, the left box plot represents the values obtained from 19 different determinations as shown in Figure 6. The right box plot represents the estimated values from 19 resampled data sets from one typical experiment.

function but is better described by a double-exponential function, particularly evident at voltages below -100 mV in 140 mM external K^+ . The time constants and their voltage dependence are in the range expected for the slow and intermediate characteristic time constants of Schemes VII and VIII.

The occurrence of the C_i state after opening is also expected to have an additional effect on the macroscopic activation kinetics. Because the rates of entry and exit from the C_i state in both Schemes VII and VIII are slower than the activation process at voltages greater than 0 mV, this state will behave like a nonabsorbing inactivated state. During voltage pulses to these depolarized voltages, therefore, we would expect to see a small ($\sim 10\%$) decline in the peak current with a time constant of about 2 to 3 ms. As shown in the following paper (Zagotta et al., 1994), this decline is generally

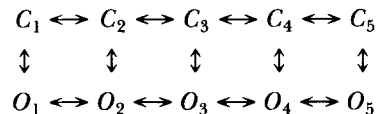
not observed. However if the channel can also enter the C_i state, or a state with similar kinetics, before opening, the models predict very little, if any, decline. While we have demonstrated that the C_i state cannot always be traversed in the process of channel activation, it can still occur as a branch off of the activation pathway. Therefore, a small fraction of the channels might enter the C_i state before opening, and thereby reduce or eliminate the predicted decline of the current.

The occurrence of the short closures after opening was first observed in voltage-dependent potassium channels from squid axons by Conti and Neher (Conti and Neher, 1980). They noted that these closures were not expected from the Hodgkin and Huxley model for potassium currents (Hodgkin and Huxley, 1952) and tentatively proposed a sequential model, essentially identical to Scheme IV, whereby the short-lived closed state is in the activation pathway. Since then, a number of investigators have observed a voltage-independent bursting behavior in potassium channels (e.g., Cooper and Shrier, 1985; Kasai, Kameyama, Yamaguchi, and Fukuda, 1986; Koren et al., 1990; Solc and Aldrich, 1990; Spruce, Standen, and Stanfield, 1989; Standen, Stanfield, and Ward, 1985; Zagotta and Aldrich, 1990*b*). Zagotta and Aldrich (Zagotta and Aldrich, 1990*b*) and Koren et al. (Koren et al., 1990) explained this bursting behavior in Shaker and RCK1 potassium channels respectively by a final voltage-independent transition in the activation pathway following four independent and identical voltage-dependent transitions. These models also can be reduced to Scheme IV where C_f is in the activation pathway. Zagotta and Aldrich (Zagotta and Aldrich, 1990*b*) argued that a model with a voltage-dependent closing transition, such as Scheme V, would produce voltage-dependent open durations at depolarized voltages if the closing transition conformed to Hodgkin and Huxley kinetics (Hodgkin and Huxley, 1952). Therefore they concluded that the burst closed state, C_f , must be in the activation pathway, as in Scheme IV. In the current study we show that the open durations are indeed voltage dependent, but at considerably more hyperpolarized voltages. Furthermore the voltage dependence conforms to the predictions of a model containing two closing transitions, a voltage-independent and a voltage-dependent transition, suggesting that transitions to C_f are separate from the activation pathway, as in Scheme V. As will be shown in the following paper (Zagotta et al., 1994), the voltage-dependence of the open durations occurs at hyperpolarized voltages because the first closing transition to the activation pathway is slower than expected from Hodgkin and Huxley kinetics.

While we have shown that the C_f state is probably not in the pathway for channel deactivation we cannot rule out the possibility that it is still in the pathway for activation. Scheme VI shows one mechanism for how this could come about. In this model the channel enters the C_f state in the process of opening at depolarized voltages but, at hyperpolarized voltages, closes directly to the . . . C state (s). A model with these essential features has recently been proposed to account for the effects of solvent on the activation time course, but not the time course of deactivation, reactivation, or gating currents (Rayner, Starkus, Ruben, and Alicata, 1992).

A model has recently been suggested for activation of voltage-dependent calcium and potassium channels that contains a state similar to C_f that is in the activation pathway but not in the deactivation pathway (Greene and Jones, 1993; Marks and Jones, 1992). This model is reminiscent of the mechanism of allosteric interaction

proposed by Monod, Wyman, and Changeux (Monod, Wyman, and Changeux, 1965). In this model the activation process of the channel involves both a conformational change in each of its subunits and a concerted conformational change that is promoted by the transitions in each subunit. This model can be summarized by the following scheme:



SCHEME IX

where C_1 to C_5 represent closed conformations after 0 to 4 subunit transitions, respectively, and O_1 to O_5 represent open conformations after 0 to 4 subunit transitions and one concerted opening transition. At depolarized voltages the voltage-independent transitions between O and Cf might represent the concerted transition between O_5 and C_5 . Since the channel will frequently activate via C_5 at depolarized voltages, this would place the Cf state in the activation pathway. However, during deactivation at hyperpolarized voltages, the channel will frequently undergo the voltage-dependent $O_5 \rightarrow O_4$ transition without entering C_5 . A mechanism like this would produce an apparent voltage-dependent closing rate (Marks and Jones, 1992), as observed. However, as we will show in the third paper (Zagotta et al., 1994), this particular form of the model is inconsistent with the voltage dependence and kinetics of activation.

The molecular mechanism that underlies the Cf and Ci states remains unclear. As indicated above the Cf \rightarrow O transition might represent a voltage-independent transition in each subunit or a concerted transition that is promoted by voltage-dependent conformational changes in each subunit, such as the T to R switch in hemoglobin (Monod et al., 1965). However this mechanism could not account for the Ci state, which cannot be in a direct line in the activation pathway. The Cf and/or Ci states could also be due to an open channel block by ions in the solution. The relative lack of voltage dependence, though, would indicate that these blocking ions could not appreciably enter the membrane electric field. Further understanding of the molecular properties of these closed conformations could come from the study of alterations in their biophysical properties by mutagenesis of the channel protein.

We thank Tom Middendorf and Max Kanevsky for helpful comments on the manuscript.

This work was supported by a grant from National Institutes of Health (NS23294) and by a National Institute of Mental Health Silvio Conte Center for Neuroscience Research Grant (MH 48108). W. N. Zagotta is a Warner-Lambert fellow of the Life Sciences Research Foundation. R. W. Aldrich is an investigator with the Howard Hughes Medical Institute.

Original version received 13 May 1993 and accepted version received 27 August 1993.

REFERENCES

- Aldrich, R. W., D. P. Corey, and C. F. Stevens. 1983. A reinterpretation of mammalian sodium channel gating based on single channel recording. *Nature*. 306:436-441.
- Armstrong, C. M. 1981. Sodium channels and gating currents. *Physiological Reviews*. 61:644-683.

- Bezánilla, F. 1985. Gating of sodium and potassium channels. *Journal of Membrane Biology*. 88:97–111.
- Blatz, A. L., and K. L. Magleby. 1986. Correcting single channel data for missed events. *Biophysical Journal*. 49:967–980.
- Cahalan, M. D., K. G. Chandy, T. E. DeCoursey, and S. Gupta. 1985. A voltage-gated potassium channel in human T lymphocytes. *Journal of Physiology*. 358:197–237.
- Catterall, W. A. 1986. Molecular properties of voltage-sensitive sodium channels. *Annual Review of Biochemistry*. 55:953–985.
- Catterall, W. A. 1992. Cellular and molecular biology of voltage-gated sodium channels. *Physiological Reviews*. 72:S15–48.
- Cole, K. S., and J. W. Moore. 1960. Potassium ion current in the squid giant axon: dynamic characteristic. *Biophysical Journal*. 1:1–14.
- Colquhoun, D., and A. G. Hawks. 1983. The principles of the stochastic interpretation of ion-channel mechanisms. In *Single-Channel Recording*. B. Sakmann and E. Neher, editors. Plenum Publishing Corp., New York. 135–175.
- Colquhoun, D., and F. J. Sigworth. 1983. Fitting and statistical analysis of single-channel records. In *Single-Channel Recording*. B. Sakmann and E. Neher, editors. Plenum Publishing Corp., New York. 191–263.
- Conti, F., and E. Neher. 1980. Single channel recordings of K⁺ currents in squid axons. *Nature*. 285:140–143.
- Cooper, E., and A. Shrier. 1985. Single-channel analysis of fast transient potassium currents from rat nodose neurones. *Journal of Physiology*. 369:199–208.
- Durell, S. R., and H. R. Guy. 1992. Atomic scale structure and functional models of voltage-gated potassium channels. *Biophysical Journal*. 62:238–250.
- Gautam, M., and M. A. Tanouye. 1990. Alteration of potassium channel gating: molecular analysis of the *Drosophila* Sh5 mutation. *Neuron*. 5:67–73.
- Gilly, W. F., and C. M. Armstrong. 1982. Divalent cations and the activation kinetics of potassium channels in squid giant axons. *Journal of General Physiology*. 79:965–996.
- Greenblatt, R. E., Y. Blatt, and M. Montal. 1985. The structure of the voltage-sensitive sodium channel. Inferences derived from computer-aided analysis of the *Electrophorus electricus* channel primary structure. *FEBS Letters*. 193:125–134.
- Greene, K. J., and S. W. Jones. 1993. An allosteric model for the delayed rectifier potassium current of frog sympathetic neurons. *Biophysical Journal*. 64:312a. (Abstr.)
- Guy, H. R., and P. Seetharamulu. 1986. Molecular model of the action potential sodium channel. *Proceedings of the National Academy of Sciences, USA*. 83:508–512.
- Hamill, O. P., A. Marty, E. Neher, B. Sakmann, and F. J. Sigworth. 1981. Improved patch-clamp techniques for high-resolution current recording from cells and cell-free membrane patches. *Pflügers Archiv*. 391:85–100.
- Heginbotham, L., and R. MacKinnon. 1992. The aromatic binding site for tetraethylammonium ion on potassium channels. *Neuron*. 8:483–491.
- Hodgkin, A. L., and A. F. Huxley. 1952. A quantitative description of membrane current and its application to conduction and excitation in nerve. *Journal of Physiology*. 117:500–544.
- Horn, R. 1987. Statistical methods for model discrimination. Applications to gating kinetics and permeation of the acetylcholine receptor channel. *Biophysical Journal*. 51:255–263.
- Hoshi, T., and R. W. Aldrich. 1988a. Gating kinetics of four classes of voltage-dependent K⁺ channels in pheochromocytoma cells. *Journal of General Physiology*. 91:107–131.
- Hoshi, T., and R. W. Aldrich. 1988b. Voltage-dependent K⁺ currents and underlying single K⁺ channels in pheochromocytoma cells. *Journal of General Physiology*. 91:73–106.

- Hoshi, T., and W. N. Zagotta. 1993. Recent advances in the understanding of potassium channel function. *Current Opinions in Neurobiology*. 3:283–290.
- Hoshi, T., W. N. Zagotta, and R. W. Aldrich. 1990. Biophysical and molecular mechanisms of *Shaker* potassium channel inactivation [see comments]. *Science*. 250:533–538.
- Hoshi, T., W. N. Zagotta, and R. W. Aldrich. 1991. Two types of inactivation in *Shaker* K⁺ channels: effects of alterations in the carboxy-terminal region. *Neuron*. 7:547–556.
- Iverson, L. E., M. A. Tanouye, H. A. Lester, N. Davidson, and B. Rudy. 1988. A-type potassium channels expressed from *Shaker* locus cDNA. *Proceedings of the National Academy of Sciences, USA*. 85:5723–5727.
- Kalbfleisch, J. G. 1985. *Statistical Inference*. Vol. 2. Springer-Verlag, New York. 360 pp.
- Kamb, A., C. J. Tseng, and M. A. Tanouye. 1988. Multiple products of the *Drosophila Shaker* gene may contribute to potassium channel diversity. *Neuron*. 1:421–430.
- Kasai, H., M. Kameyama, K. Yamaguchi, and J. Fukuda. 1986. Single transient K channels in mammalian sensory neurons. *Biophysical Journal*. 49:1243–1247.
- Kavanaugh, M. P., R. S. Hurst, J. Yakel, M. D. Varnum, J. P. Adelman, and R. A. North. 1992. Multiple subunits of a voltage-dependent potassium channel contribute to the binding site for tetraethylammonium. *Neuron*. 8:493–497.
- Koren, G., E. R. Liman, D. E. Logothetis, G. B. Nadal, and P. Hess. 1990. Gating mechanism of a cloned potassium channel expressed in frog oocytes and mammalian cells. *Neuron*. 4:39–51.
- Lichtinghagen, R., M. Stocker, R. Wittka, G. Boheim, W. Stuhmer, A. Ferrus, and O. Pongs. 1990. Molecular basis of altered excitability in *Shaker* mutants of *Drosophila melanogaster*. *Embo Journal*. 9:4399–4407.
- Liman, E. R., P. Hess, F. Weaver, and G. Koren. 1991. Voltage-sensing residues in the S4 region of a mammalian K⁺ channel. *Nature*. 353:752–756.
- Liman, E. R., J. Tytgat, and P. Hess. 1992. Subunit stoichiometry of a mammalian K⁺ channel determined by construction of multimeric cDNAs. *Neuron*. 9:861–871.
- Lopez, G. A., Y. N. Jan, and L. Y. Jan. 1991. Hydrophobic substitution mutations in the S4 sequence alter voltage-dependent gating in *Shaker* K⁺ channels. *Neuron*. 7:327–336.
- MacKinnon, R. 1991. Determination of the subunit stoichiometry of a voltage-activated potassium channel. *Nature*. 350:232–235.
- Marks, T. N., and S. W. Jones. 1992. Calcium currents in the A7r5 smooth muscle-derived cell line. An allosteric model for calcium channel activation and dihydropyridine agonist action. *Journal of General Physiology*. 99:367–390.
- Matteson, D. R., and R. J. Swenson. 1986. External monovalent cations that impede the closing of K channels. *Journal of General Physiology*. 87:795–816.
- McCormack, K., M. A. Tanouye, L. E. Iverson, J. W. Lin, M. Ramaswami, T. McCormack, J. T. Campanelli, M. K. Mathew, and B. Rudy. 1991. A role for hydrophobic residues in the voltage-dependent gating of *Shaker* K⁺ channels. *Proceedings of the National Academy of Sciences, USA*. 88:2931–2935.
- Monod, J., J. Wyman, and J. P. Changeux. 1965. On the nature of allosteric transitions: a plausible model. *Journal of Molecular Biology*. 12:88–118.
- Noda, M., T. Ikeda, H. Suzuki, H. Takeshima, T. Takahashi, M. Kuno, and S. Numa. 1986. Expression of functional sodium channels from cloned cDNA. *Nature*. 322:826–828.
- Noda, M., S. Shimizu, T. Tanabe, T. Takai, T. Kayano, T. Ikeda, H. Takahashi, H. Nakayama, Y. Kanaoka, N. Minamino, K. Kangawa, H. Matsuo, M. A. Raftery, T. Hirose, S. Inayama, H. Hayashida, T. Miyata, and S. Numa. 1984. Primary structure of *Electrophorus electricus* sodium channel deduced from cDNA sequence. *Nature*. 312:121–127.

- Papazian, D. M., L. C. Timpe, Y. N. Jan, and L. Y. Jan. 1991. Alteration of voltage-dependence of *Shaker* potassium channel by mutations in the S4 sequence. *Nature*. 349:305–310.
- Perozo, E., D. M. Papazian, E. Stefani, and F. Bezanilla. 1992. Gating currents in *Shaker* K⁺ channels. Implications for activation and inactivation models. *Biophysical Journal*. 62:160–171.
- Pongs, O., N. Kecskemethy, R. Muller, J. I. Kraus, A. Baumann, H. H. Kiltz, I. Canal, S. Llamazares, and A. Ferrus. 1988. *Shaker* encodes a family of putative potassium channel proteins in the nervous system of *Drosophila*. *EMBO Journal*. 7:1087–1096.
- Rayner, M. D., J. G. Starkus, P. C. Ruben, and D. A. Alicata. 1992. Voltage-sensitive and solvent-sensitive processes in ion channel gating. Kinetic effects of hyperosmolar media on activation and deactivation of sodium channels. *Biophysical Journal*. 61:96–108.
- Salkoff, L., K. Baker, A. Butler, M. Covarrubias, M. D. Pak, and A. Wei. 1992. An essential 'set' of K⁺ channels conserved in flies, mice and humans. *Trends in Neurosciences*, 15:161–166.
- Schoppa, N. E., K. McCormack, M. A. Tanouye, and F. J. Sigworth. 1992. The size of gating charge in wild-type and mutant *Shaker* potassium channels. *Science*. 255:1712–1715.
- Schwarz, T. L., B. L. Tempel, D. M. Papazian, Y. N. Jan, and L. Y. Jan. 1988. Multiple potassium-channel components are produced by alternative splicing at the *Shaker* locus in *Drosophila*. *Nature*. 331:137–142. [Published erratum appears in *Nature*, April 21, 1988; 332(6166): 740.]
- Shapiro, M. S., and T. E. DeCoursey. 1991. Permeant ion effects on the gating kinetics of the type I potassium channel in mouse lymphocytes. *Journal of General Physiology*. 97:1251–1278.
- Sigworth, F. J., and S. M. Sine. 1987. Data transformations for improved display and fitting of single-channel dwell time histograms. *Biophysical Journal*. 52:1047–1054.
- Solc, C. K., and R. W. Aldrich. 1990. Gating of single non-*Shaker* A-type potassium channels in larval *Drosophila* neurons. *Journal of General Physiology*. 96:135–165.
- Spruce, A. E., N. B. Standen, and P. R. Stanfield. 1989. Rubidium ions and the gating of delayed rectifier potassium channels of frog skeletal muscle. *Journal of Physiology*. 411:597–610.
- Standen, N. B., P. R. Stanfield, and T. A. Ward. 1985. Properties of single potassium channels in vesicles formed from the sarcolemma of frog skeletal muscle. *Journal of Physiology*. 364:339–358.
- Stevens, C. F. 1978. Interactions between intrinsic membrane protein and electric field. An approach to studying nerve excitability. *Biophysical Journal*. 22:295–306.
- Stuhmer, W., F. Conti, H. Suzuki, X. D. Wang, M. Noda, N. Yahagi, H. Kubo, and S. Numa. 1989. Structural parts involved in activation and inactivation of the sodium channel. *Nature*. 339:597–603.
- Stuhmer, W., and A. B. Parekh. 1992. The structure and function of Na⁺ channels. *Current Opinions in Neurobiology*. 2:243–246.
- Tempel, B. L., D. M. Papazian, T. L. Schwarz, Y. N. Jan, and L. Y. Jan. 1987. Sequence of a probable potassium channel component encoded at *Shaker* locus of *Drosophila*. *Science*. 237:770–775.
- Timpe, L. C., Y. N. Jan, and L. Y. Jan. 1988. Four cDNA clones from the *Shaker* locus of *Drosophila* induce kinetically distinct A-type potassium currents in *Xenopus* oocytes. *Neuron*. 1:659–667.
- Timpe, L. C., T. L. Schwarz, B. L. Tempel, D. M. Papazian, Y. N. Jan, and L. Y. Jan. 1988. Expression of functional potassium channels from *Shaker* cDNA in *Xenopus* oocytes. *Nature*. 331:143–145.
- Tsien, R. W., P. T. Ellinor, and W. A. Horne. 1991. Molecular diversity of voltage-dependent Ca²⁺ channels. *Trends in Pharmacological Sciences*. 12:349–354.
- Tytgat, J., and P. Hess. 1992. Evidence for cooperative interactions in potassium channel gating. *Nature*. 359:420–423.
- White, M. M., and F. Bezanilla. 1985. Activation of squid axon K⁺ channels. Ionic and gating current studies. *Journal of General Physiology*. 85:539–554.

- Young, S. H., and J. W. Moore. 1981. Potassium ion currents in the crayfish giant axon. Dynamic characteristics. *Biophysical Journal*. 36:723–733.
- Zagotta, W. N., and R. W. Aldrich. 1990a. Alterations in activation gating of single *Shaker* A-type potassium channels by the Sh5 mutation. *Journal of Neuroscience*. 10:1799–1810.
- Zagotta, W. N., and R. W. Aldrich. 1990b. Voltage-dependent gating of *Shaker* A-type potassium channels in *Drosophila* muscle. *Journal of General Physiology*. 95:29–60.
- Zagotta, W. N., M. S. Brainard, and R. W. Aldrich. 1988. Single-channel analysis of four distinct classes of potassium channels in *Drosophila* muscle. *Journal of Neuroscience*. 8:4765–4779.
- Zagotta, W. N., T. Hoshi, and R. W. Aldrich. 1989. Gating of single *Shaker* potassium channels in *Drosophila* muscle and in *Xenopus* oocytes injected with *Shaker* mRNA. *Proceedings of the National Academy of Sciences, USA*. 86:7243–7247.
- Zagotta, W. N., T. Hoshi, and R. W. Aldrich. 1990. Restoration of inactivation in mutants of *Shaker* potassium channels by a peptide derived from ShB [see comments]. *Science*. 250:568–571.
- Zagotta, W. N., T. Hoshi, and R. W. Aldrich. 1994. *Shaker* potassium channel gating III: evaluation of kinetic models for activation. *Journal of General Physiology*. 103:321–362.
- Zagotta, W. N., T. Hoshi, J. Dittman, and R. W. Aldrich. 1994. *Shaker* potassium channel gating II: transitions in the activation pathway. *Journal of General Physiology*. 103:279–319.